Vortex Ring Formation Characteristics in Synthetic Jet due to Changes of Excitation Frequency in the 1⁄2-Ball Cavity Actuator

by Ramon Trisno_4

Submission date: 14-Oct-2019 10:03PM (UTC+0700)
Submission ID: 1192571355
File name: ortex_Ring_Formation_Characteristics_in_Synthetic_Jet_due_to.pdf (941.3K)
Word count: 4888
Character count: 23589

Vortex Ring Formation Characteristics in Synthetic Jet due to Changes of Excitation Frequency in the ½-Ball Cavity Actuator

Vortex Ring Formation Characteristics in Synthetic Jet due to Changes of Excitation Frequency in the ½-Ball Cavity Actuator

Ramon Trisno[1,a*], Harinaldi[2,b*] and Engkos A. Kosasih[3,c]
[1]Mechanical Engineering Department, Faculty of Engineering, University of Pancasila, Jagakarsa, Jakarta 12640, Indonesia
[2,3]Mechanical Engineering Department, University of Indonesia, Depok, West Java, Indonesia 16424
E-mail : [a]ramontrisno@gmail.com, [b]harinald@eng.ui.ac.id, [c]kosri@eng.ui.ac.id

Abstract. A jet flow that contains vortex ring has a large energy compared to a regular jet. As one of the causes of the aerodynamic drag to the vehicle, the flow separation that occurs behind the bluff body must be controlled, so that aerodynamic drag can be significantly reduced. This study is a basic work on the development of turbulent flow separation control for aerodynamic purpose, especially in the design of the vehicle body. The main objective of this study is to analyze the performance of the synthetic jet (SJA) as one of flow control tool to reduce separation area.
To get the maximum performance of the synthetic jet actuator, the research starts by characterizing the actuator. Characterization of ½ ball-shaped cavity is done with excitation frequency changes and orifice diameter of 3, 5 and 8 mm. The study was conducted using computational and experimental methods. The experimental data was obtained by testing synthetic jet actuator with providing sinusoidal signal to drive the membrane and at the orifice end a hotwire probe that is set and plugged into a CTA (Constant Temperature Anemometry) to obtain the speed velocity of the exhaust jet. Computational methods used a commercial CFD software (FLUENT 6.3) with a Reynolds Stress Model as a model of turbulence. Each of these calculations or measurements was conducted under the same conditions.
The research result is displayed in frequency testing curve to get the maximum velocity of the jet stream. The results are further indicative of the synthetic jet actuator capability to generate vortex rings. In the experimental results, the determination of ring vortex formation taken from the calculation of the flow velocity, while the CFD simulations, the formation of vortex rings can be seen from the visualization of the flow contour. Vortex ring formed from this ½ -ball cavity, occurred at 3 mm and 5 mm orifice diameter, while the 8 mm orifice diameter cavity cannot form a ring vortex.

Keyword: synthetic jet actuators, reversed Ahmed body, vortex ring, bluff body

1. Introduction

The latest research in vehicle aerodynamics is carried out with a design standpoint related to fuel economy. For this reason, ground vehicle aerodynamics have been studied experimentally and numerically by many researchers. Most previous studies have used simple models of vehicles that can generate relevant features of the flow around a real vehicle [1] [2] [3] [4] [5] [6]. The wake around the flow field is characterized by a pair of horseshoe vortices and trailing vortices which comes from the edge of the sloping side of the body

Experiments of passive flow control in the wind tunnel model or prototype vehicle has been widely performed in various research [7] [8]. However, passive flow control give a weak effect in vehicle aerodynamic because the properties of the flow that involved is turbulent and the contribution of friction on aerodynamic drag is still small, only about 10% [9].

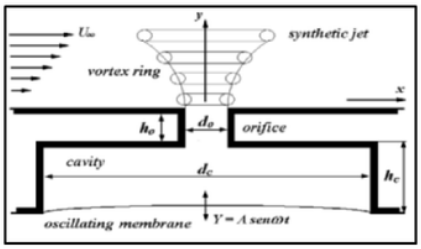

Figure 1 Sketch of a synthetic jet actuator in a cavity formed by the outlet orifice

Flow control on the bluff body in order to reduce drag and noise is one of the main issues in aerodynamics. The pressure difference between the front and the back side of the bluff body is a major contributor to the overall drag, the difference is primarily due to flow separation at the rear region of the body [10].

The need for an effective drag reduction encourage the automotive design to be more creative in developing innovative active control model. Active control method makes it possible to modify the topology of the flow without changing the shape of the vehicle. Within the scope of academic and industrial laboratories, active control methods have been developed with computational and experimental methods, and significant results have been obtained in an academic framework [7]. Suction active control that are placed on top of the rear window is able to eliminate the separation on a simplified geometry fastback cars where aerodynamic drag reduction obtained was about 17% [11]. Numerical study conducted by Kuorta and Gillieron using a synthetic jet active control placed at the top of the rear window Ahmed model showed a drag reduction of 13% [12].

Characteristics of the flow velocity on synthetic jet is taken from the center axis, U_{CL}, as the assumption of the highest velocity profile at the exit orifice. Since the spatial velocity profile can show significant deviation from the top-hat shape, a more general velocity scale is the time-and-spatially averaged exit velocity over the expulsion stroke, [13]

$$U = \frac{1}{T/2}\frac{1}{A_n}\int_{A_n}\int_0^{T/2} U(t, A_n)\,dt\,dA_n \qquad [1]$$

Where U is the average velocity of the axial phase, T is the period of excitation and A_n is the cross-sectional area of the exit nozzle.

The average velocity can be used to determine the Reynold number of the jet. The important thing at the length scale of synthetic jet flow is the stroke length L_o / D, that given by:

$$L_o = \int_0^{T/2} U_{ave}(t)\,dt \qquad [2]$$

U_{ave} is a spatial average flow velocity. Stroke length is the distance that the fluid taken during the pushing process as a part of the cycle. The excitation frequency f can be non-dimensionalized as a Stokes number, S, that given by :

$$S = \sqrt{\frac{2\pi f D^2}{\nu}} \qquad [3]$$

The non-dimensional parameter uniquely determines the operating conditions of the synthetic jet and greatly affects its ability to transfer linear momentum. In particular, Holman et al. [19] showed that in order to achieve vortex escape after the expulsion stroke (defined as synthetic jet formation)

$$\frac{\mathrm{Re}_U}{S^2} > C \qquad [4]$$

where C is a constant which equal to 0.16 for the axis symmetric and equal to 1 for the rectangular nozzles. According Utturkar et al [14] [15], the condition for a vortex ring to be formed is $Re_U / S^2 > 1$. Meanwhile, according to Smith and Swift opine the ring vortex can occur if: [16] [17] [18]

$$\frac{L_0}{D} = St > 6 \qquad [5]$$

The purpose of this study was to obtain the characteristics of the SJA with half ball-shaped cavity by providing the oscillation frequency of the membrane, in order to obtain the best performance from changes in the diameter of the orifice in the cavity.

2. Experiment Settings

Before starting the study of synthetic jet performance to the drag reduction on the vehicle, it need to know about the performance of SJA itself, in order to get the maximum results for drag reduction. The purpose of this research on the performance of SJA is to choose the type of actuator that is good in forming vortex ring during the operation of SJA. Selection was based on the SJA actuator cavity shape, orifice diameter and comparison of performance through experiments and CFD simulations. In this research, ½ ball cavity shape was studied with a diameter of 3 mm (B3), 5 mm (B5) and 8 mm (B8) (Figure 2).

Figure 3 is a schematic diagram of the synthetic jet performance test through the experiment. Synthetic jet component consisted of cavity and *piezoelectric* membrane component, mounted as a whole and driven by the function generator. This tool unleashed the desired wave signal. A signal which used in this experiment was a sinusoidal wave. The movement of the membrane made the air pushed out of the cavity and sucked into the cavity back. This tool had

a mechanical system with a very small mass with the stem and the spring move. This mass was hanged just two microns (two millionths of a meter) from the electronic circuit.

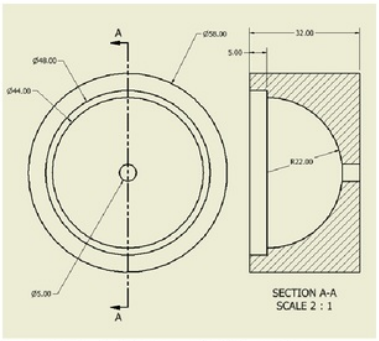

Figure 2. ½ -ball shaped SJA cavity

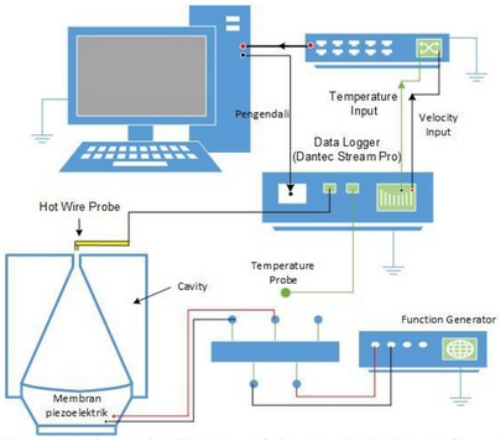

Figure 3 schematic diagram of the synthetic jet performance testing

Figure 4 Piezoelectric

Furthermore, the speed of the air that come out of this cavity through the orifice was measured using a hot wire probe 55P14 Gold Plate. This single wire probe had a wire diameter d_w = 5 μm and the distance of the branch 1.2 mm, placed on a SJA as near as possible, in this case the possible distance was equal to ± 0.5 mm above the orifice of synthetic jet actuator, so that the movement of the probe along the axis x did not touch the cavity. These probes were connected to the Data Logger, brand DANTEX Stream pro, type 91C10, CTA module that served to record the incoming data from hotwire in the form of low voltage. Then the data was entered into the tool Data Acquisition Board of National Instrument BNC-2110. This tool was used to change the analog data into digital data. The tool was connected to the computer via a data cable. This computer was also connected to a data logger which serves to control the speed of recording desired data. Before recording the data, the probe had to be calibrated using a calibration unit Dantec Streamline Pro Automatic Calibrator System S / N 9091H0013445 and King's Law that suitable for the job to interpret the data speed below the calibration range. The range of the calibration performed at 0.02 ÷ 30 m / s before each experiment performed. The calculation result of uncertainty due to calibration for all data retrieval speed was about 2.5%. Radial velocity profile was measured with a hot wire probe which across the hole using the tool transfer (vise) and the displacement distance was measured using a dial indicator with 0.01 mm accuracy.

Velocity data collection procedure was done under two conditions. The first was the velocity measurement for determining the frequency that produces the maximum speed. The process of data collection was intended to get the maximum speed that can be generated SJA and the amount of data allowed (uncertainty) by varying the sinusoidal frequency issued by the function generator. The given frequency is 20 Hz ÷ 200 Hz. Data taken as much as 60,000 data at a data rate of 30,000 data/s. The second procedure was the jet velocity measurements at points determined by the Cartesian coordinates (*X/D*, *Y/D*). This jet velocity was measured only in the half part region, because the jet was considered symmetrically formed. The value of *X/D* is 0, 0.25, 0.5, 0.75, ... ,4, while the value of *Y/D* is 0, 1, 2, 3, ... , 10. Velocity data were recorded at 10,000 data/s for 6 seconds.

The purpose of this simulation was to compare the results obtained with the results of experiments conducted as well as to visualize the vortex ring that formed by SJA. The test condition used in the experiment was similar to that used in the CFD simulation. Determination of the frequency used in CFD simulations are based on experimental results that were achieved, such that the use of User Defined Function (UDF) in the simulation matched with experimental results.

Simulations performed using software FLUENT computational fluids dynamic software version 6.3.2.6 and Gambit version 2.4.6 to form geometry, defining the role of the components, and define meshing. Meshing is used for CFD simulations in the study had determined its density is coarse (5000 mesh), intermediate (20 000 mesh) and fine (60 000 mesh). Mesh independencies done to find amount of mesh are most suitable for use in the simulation of fluid flow as well as the convergence correcting numerical calculation by computer. This study uses two approaches to mesh independencies. First, look for the minimum total error with the same parameters on the frequency and the same wavelength as well as at 1 time step using the turbulence models of Reynolds Stress Model. Second, match the simulation results (using the turbulence models of Reynolds Stress Model) with experimental results. Mesh is closest to the result of experiments that would be used for computational stages.

Turbulence models is a computational procedure for calculating the main equations of flow with a certain flow conditions. To obtain the solution of turbulent flow, the flow should be modeled mathematically. Turbulence models used in this computing method is RSM (Reynolds Stress Model). The Reynolds stress model involves calculation of the individual Reynolds stresses, $\overline{u_i' u_j'}$, using differential transport equations. The individual Reynolds stresses are then used to obtain closure of the Reynolds-averaged momentum equation. The exact transport equations for the transport of the Reynolds stresses, $\rho \overline{u_i' u_j'}$, may be written as follows:

$$\frac{\partial}{\partial t}\rho\overline{u_i'u_j'} + \frac{\partial}{\partial x_k}\left(\rho u_k \overline{u_i'u_j'}\right) = -\frac{\partial}{\partial x_k}\left[\rho\overline{u_i'u_j'u_k'} + \overline{p}\left(\delta_{kj}u_i' + \delta_{ki}u_j'\right)\right]$$
$$+\frac{\partial}{\partial x_k}\left[\mu\frac{\partial}{\partial x_k}\left(\overline{u_i'u_j'}\right)\right] - \rho\left(u_i'u_k'\frac{\partial u_j}{\partial x_k} + u_j'u_k'\frac{\partial u_i}{\partial x_k}\right) - \rho\beta\left(g_i u_j'\theta + g_j u_i'\theta\right)$$
$$+\overline{p\left(\frac{\partial u_i'}{\partial x_j} + \frac{\partial u_j'}{\partial x_i}\right)} - 2\mu\overline{\frac{\partial u_i'}{\partial x_k}\frac{\partial u_j'}{\partial x_k}} - 2\rho\Omega_k\left(\overline{u_j'u_m'}\in_{ikm} + \overline{u_i'u_m'}\in_{jkm}\right) + S_{user} \qquad [6]$$

3. Results and Discussion

3.1 Frequency Testing and Mesh Independencies

The early stages of the experiment was to determine the frequency that can produce a maximum flow rate so that the performance of this SJA as a reference in subsequent experiments. This testing is done by varying the frequency of the wave with function generator tool which use sinusoidal wave.

The test results on the SJA frequency shows that the type B3 and B8 experience the maximum velocity at the frequency of 120 Hz, while at the B5, maximum velocity occurs at a frequency of 130 Hz. The flow velocity produced by SJA types B3 is higher than other types of SJA, where the average jet velocity is equal to 7.786 m / s.

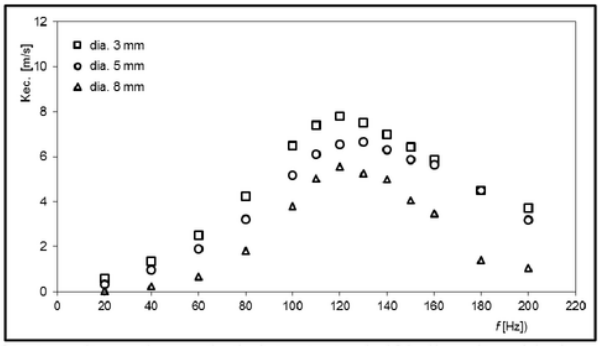

Figure 5. The graph of test results on the synthetic jet actuator half-ball cavity with sinusoidal amplitude types.

In the computational study, meshing testing needs to be done in advance, using software Gambit 2.4.6. This meshing testing aims to get the meshing residues that are not changed to deformation and meshing journals. Then the predefined meshing is used later as input material in CFD simulation processing. The type of the cavity and orifice diameter adapted to the experimental conditions. Each meshing is then processed using software *Fluent 6.3.26*. Conditions of iterations taken on the position of $X/D = 0$ and $Y/D = 0$ with 200 data at the speed of data recording 10,000/s.

To determine the certainty and reliability of the data obtained from the experiment, the uncertainty values used in the equation below, applies for a confidence level of 95%, given by:

$$U_x \propto \sigma_{\bar{x}} \Rightarrow U_x \approx k(convidence\ limit)\,\sigma_{\bar{x}}$$

$$\sigma_{\bar{x}} = \frac{2S_x}{\sqrt{N}} \qquad [7]$$

As for determining the percentage level of measurement uncertainty (U_x), the following equation was used:

$$U_x = \frac{\sigma_{\bar{x}}}{\bar{x}} \times 100\% \qquad [8]$$

The calculation of uncertainty in each cavity was taken based on the number of sampling data. The data are processed on the condition $Y/D = 0$ and $X/D = 0$, the point (0,0) which is the onset of the synthetic jet. This point has a greater uncertainty value than the other points.

For first 10,000 data, uncertainty calculation using equations [7] and [8], the uncertainty calculation result in B3 cavity type at 1.61%, B5 cavity types at 1.58 % and B8 cavity types at 0.98%. Based on the value of this uncertainty, the B3 cavity type have greater uncertainty value than the other cavity types. Hence, the value of uncertainty in B3 should be aware of its magnitude, so that the amount of data captured on the experimental conditions can qualify a data confidence level at 95%, then the value of the uncertainty should be below 5%. But the results of the calculations shows that the data obtained by the experimental method provides that the uncertainty value does not exceed 2%. The value is below the required value.

3.2 Average Jet Velocity

Membrane on synthetic jet actuator (SJA) oscillates with a sinusoidal frequency, so that the SJA generates air flow out through the orifice. The orifice tip, i.e. the (0,0) point experienced a higher air flow rate compared to other points. U_{CL} is the airflow velocity at the point (0,0) coming out form the of the tip orifice, while U_x is the local air flow rate at a certain point.

Figure 6 is a comparison of U_x/U_{CL} at the point (0,0) produced by synthetic jet actuator with a half-ball cavity shaped and orifice diameter of 3 mm (B3). The left graph is an experimental results graph, while the right graph is a CFD simulation results graph. Both of these graphs looks similar in the data distribution. On the $0 < X/D < 1$, it appears that the value of U_x/U_{CL} is above 0.2. This means at the $0 < X/D < 1$ condition, the velocity of the jet flow is high. While at the $1 < X/D < 2$, the value of the speed ratio U_x/U_{CL} decreased quite dramatically, so that the possible occurrence of velocity difference is quite large in this area. The author notes, that in regions $1 < X/D < 2$ there has been a flow separation between areas affected by jet to areas not affected by the jet. This makes it possible to form a kind of the boundary layer between the area experiencing jet to areas not affected by the jet. But for areas $2 < X/D < 4$ speed differences tend to be smaller and more constant. It is influenced by the jet center which is farther to the area. The presence of the flow velocity in the area is not caused by a jet of air that comes out of the SJA but rather caused by turbulence around the mouth of the orifice. Turbulence is caused by the collision of air flow into the cavity with the flow of air that had not sufficient time to get out. So that the air flow is partially not enter into the cavity but being around the orifice of the SJA.

Figure 7 depicts the distribution of air flow velocity at B5 obtained from experiments and CFD simulations. The graph of experimental results (7a) shows that for $0 < X/D < 2$ speed ratio U_x/U_{CL} showed a significant difference due to the change of Y/D with a value range $0.1149 < U_x/U_{CL} < 1$. The smallest value (0.1149) and the largest value (1) is located along the center line. The velocity change in the central line is experiencing considerable fluctuation. As for $2 < X/D < 4$, U_x/U_{CL} did not show a big difference. Figure 8, shows the experimental results that U_x/U_{CL} is very significant at $0 < X/D < 1$. A very sharp slope of theU_x/U_{CL} occurs in this area. It shows that the area where the jet is possibly formed is only at $0 < X/D < 1$. While at $X/D > 1$, it tends to form a horizontal chart, meaning that the speed of air flow in that region is unlikely to change significantly. Likewise with the graph from the CFD simulation results, shows similar results to the experiment. Only in $Y/D = 0$ gives a greater change of velocity compared with other Y/D.

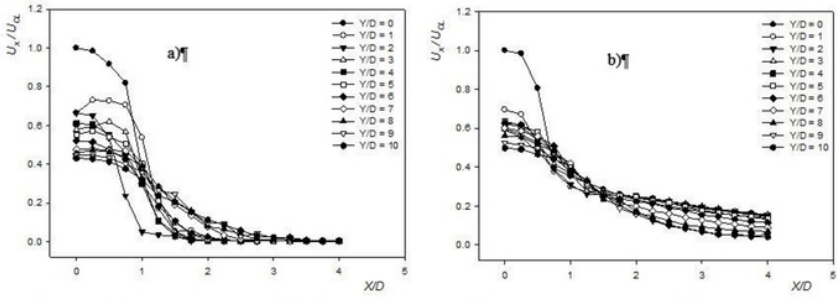

Figure 6 the comparison of U_x/U_{CL} graph on the B3, a) experiment, b) CFD simulation

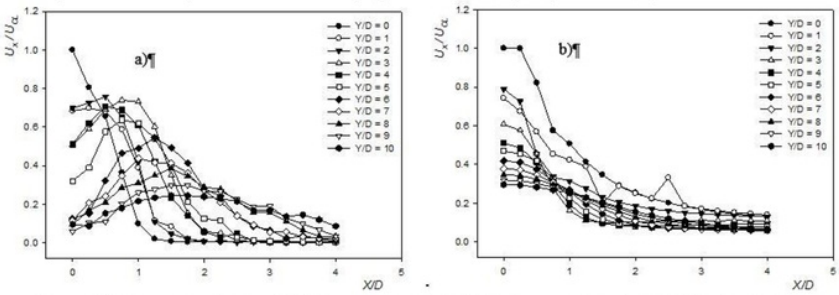

Figure 7 the comparison of U_x/U_{CL} graph on the B5, a) experiment, b) CFD simulation

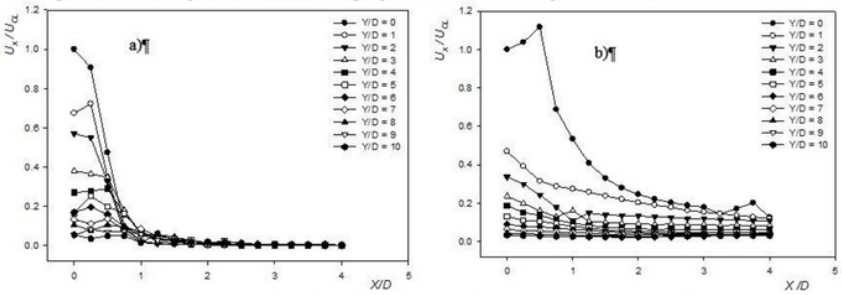

Figure 8 the comparison of U_x/U_{CL} graph on the B8, a) experiment, b) CFD simulation

3.3 Determining the occurrence of vortex Ring

When the bursts of flow come out through the orifice, the bursts is not necessarily form a vortex ring. Vortex ring formation is preferred so that the thrust of the bursts is more powerful and could protect the bursts to remain solid. The un-formation of a vortex ring can be caused by the flow rate, the frequency of the excitation and the diameter of the orifice. Jet is formed when the ratio between the Reynolds numbers with squared Stoke number is > 1 and the ratio between the stroke length and orifice diameter is > 6 filled. Here, Table 3 is the result of calculations based on equations [4] and [5] at the B3, B5 and B8 cavity model, at exactly above the orifice and with the maximum frequency.

Table 3 Results of calculation of the occurrence of vortex rings in the half ball cavity

Cavity	*Lo* [mm]	*Uo* [m/s]	Stroke ratio	Re_U/S^2	Explanation
B3	48.74	5.85	16.25	2.77	Occur
B5	26.25	3.41	5.25	0.84	Not-Occur
B8	22.25	2.67	2.78	0.44	Not-Occur

The next step is the determination of the occurrence of vortex rings on each type of cavity, and the visualization of computational simulation results can be seen in Figure 9a, 9b and 9c. Figure 9a shows the velocity contours due to

the movement of the membrane in the cavity B3. When the membrane moves at t/T = 1/8, the membrane is at blowing step, and it shows the airflow out through the orifice. Then at t/T = 1/4, the contour of the flow is beginning to show the formation of vortex rings. This position is the culmination expulsion step by the movement of the membrane. Membrane starts to move downwards and SJA perform suction step. After reaching at t/T = 3/8, then the vortex ring will be seen more clearly. Then at t/T = 1/2, the vortex ring is split off and move up. Suction step continued to stage t/T = 5/8. In this position, some of the air under the vortex ring will be sucked back into the cavity. This can affect the shape of the vortex ring which has been formed by the blowing of SJA. But on B3 cavity, the vortex ring which is formed remains intact and further intensified at t/T = 3/4. Then at t/T = 7/8, the membrane moves up, and the SJA start to blow. In this condition, the vortex ring which has been formed is ready to break away by the formation of a new vortex ring. At t/T = 1, vortex ring have released itself from the tip of the orifice.

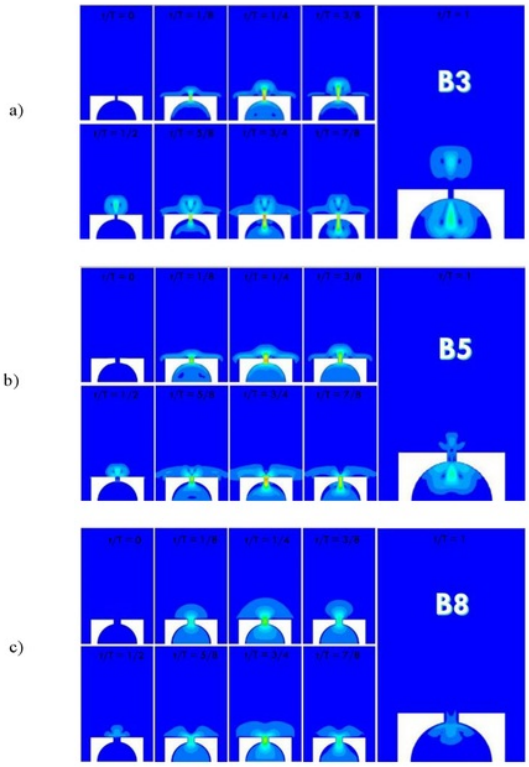

Figure 9. Formation visualization of the vortex rings at B3, B5 and B8

Figure 9b shows the velocity contours produced by B5 cavity SJA. The vortex ring began to take shape at t/T = 1/4. At t/T = 3/5, the vortex ring begin to separate from the tip of the orifice. It clearly shows that the vortex ring is leaving the tip orifice at t/T = 1/2. But when the membrane moves down at t/T = 5/8, most of the air around the mouth of the orifice began to be sucked into the cavity, and the vortex ring that has been formed over the orifice is immediately affected by the suction of SJA, as shown by the figure at t/T = 3/4. Consequently, the vortex ring is rupture (at t/T = 7/8) and failed to form, as shown at t/T = 1.

Figure 9c shows the velocity contours produced by B8 cavity SJA. In the initial condition of blow step which generated by SJA, velocity contours do not shown the formation of the vortex ring. As also at the suction conditions, at t/T = 5/8, most of the air at the end orifice, seen flowing into the cavity and filled the cavity. This situation shows that there is no vortex ring formed by the process of SJA on B8. Thus, it can be said that both method, experiment and CFD simulation give the same result.

4. Conclusion

From the results of the research on the characteristics of synthetic jet actuator, some conclusions can be taken. The frequency obtained to get the maximum velocity jet flow of B3 and B8 cavity is at 120 Hz and B5 is at 130 Hz. Based on the number of data taken, the value of uncertainty has been reached below 2%. Results of flow velocity measurements in absolute terms through experiments and CFD simulations shows near close results. Distribution of the jet stream average speed occurs higher in $X/D < 1$, then decreased after $X/D > 1$. The flow rate at absolute maximum jet streams occur on B3. In determining whether the occurrence of vortex ring due to movement of SJA, the experimental results were processed in the existing equation and the results obtained from CFD simulation, gives the same results. Vortex ring can occur only at B3, whereas at B5 and B8, SJA cannot form a vortex ring.

5. References

[1] Ahmed S.R., G. Ramm and G. Faltin., 1984, SAE paper, Detroit, Michigan, USA, 8400300-01
[2] Hintenberger C., Villalba M. G. &Rodi W., 2004, Large eddy simulation of flow around the Ahmed body, Institute for Hydromechanics, University of Karlsruhe, Germany
[3] Fares E., 2006, Unsteady flow simulation of the Ahmed reference body using a lattice Boltzmann approach, Computers and Fluids, 35, pp. 940-950
[4] Minguez M., Pasquetti R. &Serre E., 2008, High-order Large Eddy Simulation of Flow over the Ahmed Body' Car Model', Physics of Fluids, 20
[5] Uruba V., and Hladik O., 2009, On the Ahmed Body Wake, Colloquium Fluid Dynamics, Institute of Thermomechanics AS CR, v.v.i., Prague
[6] Conan B., Anthoine J., and Planquart P., 2011, Experimental Aerodynamic study of a car-type bluff body, Experimental of Fluids, 50, pp. 247 – 259
[7] Gak-El-Hak, M., 1996, Modern Development in Flow Control, Appl. Mech. Rev., 9, pp. 365-379
[8] Hucho W.H., 1998, Aerodynamics of Road Vehicle, Annu. Rev. Fluid Mech., 25, pp 285-537
[9] Kourta A. &Gillieron P., 2009, Impact of automotive Control on the Economic Issues, Journal of Applied Fluid Mechanics, vol. 2, no. 2, pp. 69 – 75
[10] Hucho W. H., 2002, Aerodynamik der stumpfer K''orper – PhysikalischeGrundlagen und Anwendung in der Praxis, Vieweg-Verlag
[11] Roumeas M., Gillieron P., and Kuorta A., 2009, Analysis and Control of near wake flow over a square back geometry, Computers & Fluids, 38, pp. 60 – 70
[12] Roumeas M., Gillieron P., and Kuorta A., 2009, Drag Reduction by Flow Separation Control on a Car after Body, International Journal for Numerical Method in Fluids, 60, pp. 1222 – 1240
[13] Feero, Mark A., Lavoie, Philippe, Sullivan, Pierre E, Influence of cavity shape on synthetic jet performance. Sensors and Actuators A: Physical 223 (2015) page 1 – 10, Elsavier, 2014.
[14] R. Holman, Y. Utturkar, R. Mittal, B.L. Smith, L. Cattafesta, Formation criterionfor synthetic jets, AIAA J. 43 (10) (2005) 2110–2116.
[15] Utturkar, Y., "Numerical Investigation of Synthetic Jet Flow Fields," M.S. Thesis, Department of Mechanical Engineering, University of Florida, 2002.
[16] Smith, B. and Glezer, A. "The formation and evolution of synthetic jets." Phys. Fluids, Vol. 10, No. 9, 1998, pp. 2281-2297
[17] Glezer, A., "The Formation of Vortex Rings," Phys. Fluids, Vol. 31, No. 12, 1998, pp. 3532-3542.
[18] Smith, B. and Swift, G. "Synthetic Jets at Large Reynolds Number and Comparison to Continuous Jets," AIAA Paper 2001-3030, 2001.

Vortex Ring Formation Characteristics in Synthetic Jet due to Changes of Excitation Frequency in the 1⁄2-Ball Cavity Actuator

ORIGINALITY REPORT

19%	12%	16%	11%
SIMILARITY INDEX	INTERNET SOURCES	PUBLICATIONS	STUDENT PAPERS

MATCH ALL SOURCES (ONLY SELECTED SOURCE PRINTED)

7%

★ B Mohan, S Mariappan. "Influence of non perfect impedance boundary on the bistable region in thermoacoustic interactions", Journal of Physics: Conference Series, 2017

Publication

Exclude quotes	On	Exclude matches	< 10 words
Exclude bibliography	On		